V International Conference on Particle-based Methods – Fundamentals and Applications
PARTICLES 2017
P. Wriggers, M. Bischoff, E. Oñate, D.R.J. Owen, & T. Zohdi (Eds)

CHARACTERIZING GAS FILM CONDUCTION FOR PARTICLE-PARTICLE AND PARTICLE-WALL COLLISIONS

Andrew M. Hobbs*‡ and Jin Y. Ooi†

* Astec, Inc.
4101 Jerome Ave.
Chattanooga, Tennessee, 37407, USA
e-mail: ahobbs@astecinc.com, web page: http://www.astecinc.com

†‡ School of Engineering, The University of Edinburgh
William Rankine Building, The King's Buildings
Thomas Bayes Road, Edinburgh, EH9 3FG, United Kingdom
e-mail: j.ooi@ed.ac.uk, web page: http://www.eng.ed.ac.uk/research/institutes/iie

Abstract

Heat transfer in granular media is an important mechanism in many industrial applications. For some applications conduction is an important mode of heat transfer. Several models have been proposed to describe particle scale conduction both between particles (particle-particle) and with walls (particle-wall). Within these conduction models are several distinct modes: conduction through physical contact (macro-contact), conduction through surface roughness (micro-contacts), and conduction through the stagnant gas film surrounding each particle (particle-fluid-particle or particle-fluid-wall). While these models have been developed and verified in literature, the relationship between the conduction heat transfer coefficient and key parameters is not immediately obvious. This is especially true for gas film conduction. In this work we investigate gas film conduction for particle-particle and particle-wall collisions via DEM simulations using a well-established gas film model to determine the behavior of the heat transfer coefficient as a function of the separation distance and particle size. With a better understanding of the gas film heat transfer coefficient, we propose a simplified model that captures the same response but is easier to understand and significantly more computationally efficient.

Keywords: Conduction, Discrete element method, gas film conduction, granular heat transfer

INTRODUCTION

Heat transfer in granular materials is a common occurrence in many industrial applications. In many instances hot gases are used to convectively heat the particles. However, there are some applications where conductive heat transfer is the dominant mode. One such application is the heating of recycled asphalt product (RAP). RAP is the millings from road surfaces and is comprised of aggregates and bitumen coating. For RAP to be reused in new road surface mixes, it must be heated and any moisture evaporated. Since the bitumen coating is flammable, a flame cannot be used to directly heat the RAP. A common method is to mix hot, uncoated (virgin) aggregate with the cold, wet RAP. In such a process conductive heat transfer between the virgin and RAP is dominant.

Numerical techniques used to simulate particle systems are now well established and increasing computational power means more industrial scale processes are accessible via methods such as the discrete element method (DEM) [1,2,3]. Since heat transfer is common in many industrial processes, particle models have been extended beyond simple contact mechanics to include thermal effects [4,5]. Coupling to a fluids solver permits convective heat transfer between the fluid and particle phase to be calculated [6,7] but this is expensive and unnecessary where convection is not dominant. A common approach where conduction is dominant is DEM particle scale simulation using the Hertzian soft sphere contact model. Conductive heat transfer was added to this approach by Batchelor and O'Brien [8]. This model assumes that heat flows through the physical contact (or macro-contact) between particles given by the Hertzian contact radius:

$$Q_{MC} = 2k^* \left[\frac{3F_N R^*}{4E^*}\right]^{1/3} \Delta T \tag{1}$$

where k^* is the effective thermal conductivity, F_N is the normal force, R^* is the effective radius, E^* is the effective Youngs modulus, and ΔT is the temperature difference.

Rong et al. [9] postulated that in addition to physical contact, conduction could occur through a stagnant gas layer surrounding each particle. As the gas film surrounding a particle touches an adjacent surface (particle or wall), conduction occurs through the gas film. The heat rate can be calculated according to Fourier's Law:

$$Q_{film} = \int \frac{dA}{\Delta L} k_f \Delta T \tag{2}$$

where k_f is the fluid thermal conductivity, A is the surface area , and ΔL is the separation distance.
It follows that the conductive heat transfer rate through particle-fluid-particle Q_{pfp} and through particle-fluid-wall Q_{pfw} can be described as follows:

$$Q_{pfp} = \int_{r_{in}}^{r_{out}} \frac{2\pi k_f}{\max(l,s)} dr\, \Delta T \tag{3}$$

$$Q_{pfw} = \int_{r_{in}}^{r_{out}} \frac{2\pi k_f r}{\max(l,s)} dr\, \Delta T \tag{4}$$

where the linear distance between particle surfaces is defined by the variable l, the radial dimension by the variable r, and the upper and lower bounds of the integral r_{out} and r_{in} are illustrated for the particle-fluid-particle contact in Figure 1. To prevent a singularity at the point of contact, a minimum limit s=2.75 x 10^{-8} m is assumed to be related to the mean free path of gas.

Rong [10] assumed that the macro-contact was analogous to the contact area separated by the mean free path of gas equation (9).

$$Q_{MC=} \frac{k_f A_c}{4.0 \times 10^{-10}} \Delta T \tag{5}$$

This approach was implemented by Bu et al. (2013) to include micro-contact surface roughness, the macro-contact and gas film model by Rong as well as the interior thermal resistance of the particle. For Biot numbers less than one, the particle can be assumed to be isothermal and the interior resistance neglected.

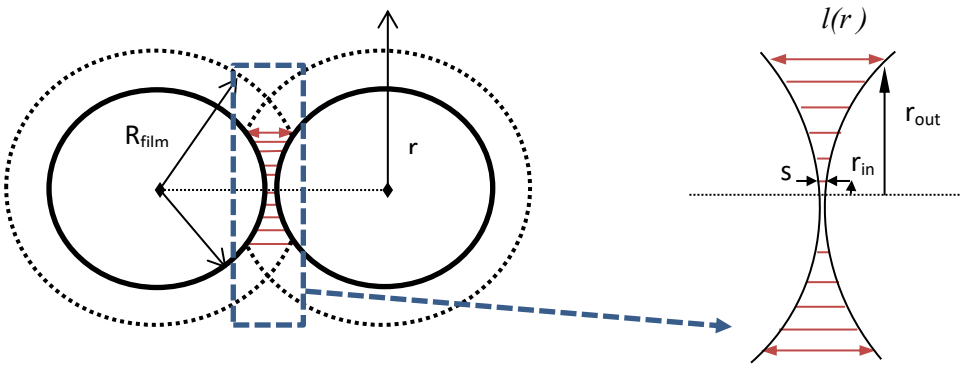

Figure 1 *Illustration of particle-fluid-particle conduction*

Morris et al. [12] combined the Rong's gas film model with the Batchelor and O'Brien's macro-contact model from Equation 1. Morris et al. also determined that for materials with a low thermal conductivity the gas film could be as much as two orders of magnitude more than the physical contact. The authors proposed a ratio to determine the effect of the gas film relative to the macro-contact, given by:

$$\frac{R_P k_f}{R_c k_P} \geq 1 \tag{6}$$

where R_P is the particle radius and R_c is the contact radius and k_f and k_p are the thermal conductivity of the fluid and particle, respectively. For values greater than one, the gas film conduction is dominant.

In this study we focus on gas film conduction for particle-particle and particle-wall collisions. Internal resistance is neglected as the effect is deemed negligible in the specific application of RAP processing. The analytic solution to the integral of Fourier's equation for sphere-sphere and sphere-wall was implemented according to the algorithm by Morris in the MFIX code. The analytic solution to particle-fluid-wall heat transfer coefficient $\widehat{H}$ is given in Equation 7 below, where the normalized particle overlap $\widehat{\delta}$ is greater or equal to zero when physical contact occurs. When $\widehat{\delta}$ is less than zero there is only gas film contact. A similar set of equations provides the solution for particle-fluid-particle contacts. The variables previously described in equations 3 and 4 are made dimensionless by dividing by the particle radius and denoted in Equation 7 by the ^ symbol.

$$\widehat{H} = \begin{cases} \frac{\pi}{\hat{s}}\left[\left(1-\hat{\delta}\right) - A^2\right] + 2\pi\left[B - A + \left(1-\hat{\delta}\right) ln\left(\frac{1-\hat{\delta}-B}{\hat{s}}\right)\right], & \hat{\delta} \geq 0 \\ 2\pi\left[\frac{\hat{r}_s^2}{2\hat{s}} + B - C + \left(1-\hat{\delta}\right) ln\left(\frac{1-\hat{\delta}-B}{1-\hat{\delta}-C}\right)\right], & \hat{\delta} < 0 \end{cases} \tag{7}$$

where

$$A = 1 - \hat{\delta} - \hat{s}$$
$$B = \sqrt{1 - \hat{r}_{out}^2}$$
$$C = \sqrt{1 - \hat{r}_s^2}$$

and

$$\hat{r}_{out} = \begin{cases} \sqrt{\hat{R}_{film}^2 - (1 - \hat{\delta})}, & \hat{\delta} < 1 - \sqrt{\hat{R}_{film}^2 - 1} \\ 1, & \hat{\delta} \geq 1 - \sqrt{\hat{R}_{film}^2 - 1} \end{cases}$$
$$\hat{r}_s = \begin{cases} \sqrt{1 - A^2}, & \hat{\delta} > -\hat{s} \\ 0, & \hat{\delta} \leq -\hat{s} \end{cases}$$

Whilst these models have been developed and verified to a limited extent, the relationship between the conduction heat transfer coefficient and the key parameters is rather obscure. This is especially true for gas film conduction which is dominant in many industrial processes where the industrial solids are poor conductors such as in this study on RAP and road aggregates. In this study we investigate the gas film conduction for particle-particle and particle-wall collisions via DEM simulations to determine the behavior of the heat transfer coefficient as a function of the separation distance and particle size.

Gas Film Conduction For Poly-dispersed Particle Systems

The Rong gas film conduction model assumes that the gas film thickness is roughly 50% of the particle radius. Morris showed that the solution is not especially sensitive to this value and proposed a value of 42%. In this work we use a gas film thickness that is 40% of the particle radius. Because the integral solution to Fourier's equation is dependent on the linear distance from one particle surface to the other particle (or wall) surface, the minimum size ratio for this to remain valid is 0.4 (see Figure 2). The means the smaller particle's radius cannot be smaller than the larger particle's film thickness, otherwise the film thickness could enclose some surface area of the smaller particle not in direct line with the larger particle. With this limitation in mind and assuming fixed material properties for spherical particles, the gas film heat transfer coefficient should be related only to the particle size ratio and separation distance.

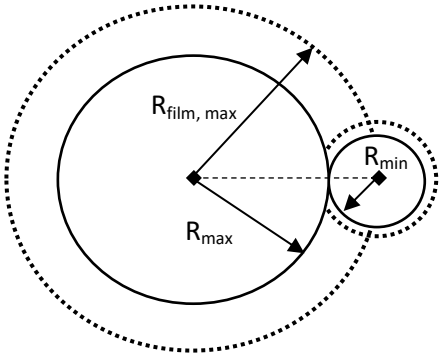

$$R_{min} \geq R_{film,max} - R_{max}$$

Figure 2 *Illustration of minimum size ratio where $R_{min} \geq$ film thickness*

NUMERICAL METHODS: DEM SIMULATIONS

Particle-Particle Collisions

The Rong gas film model as implemented by Morris in the open source multiphase code MFIX [12,13] was implemented as a custom contact model in the commercial DEM code EDEM [14]. Care was taken to use as near to the original Morris algorithm as possible although some minor changes were necessary due to differences in which variables were directly accessible from each DEM solver. Particle-particle and particle wall collisions were investigated using the Rong/Morris models for a range of particle size ratios varying from 1 to 0.4. Table 1 shows the material properties and simulation settings. Two particles with the same material properties were slowly brought into contact. The simulated velocities were very low and the resulting minimal collision force meant that the influence of physical contact could be neglected. The gas film heat transfer coefficient was calculated from the predicted heat flux and temperature difference. Figure 3 shows some representative results at the point of contact.

Table 1 Material properties and simulation settings used in DEM simulation

Density	2500 kg/m^3
Young's Modulus	5.0 x 10^{10} Pa
Poisson's Ratio	0.3
Thermal Conductivity	0.96 W/m K
Specific Heat	472 J/kg K
Coefficient of Restitution	1 x 10^{-7}
Coefficient of Static Friction	0.5
Particle Radius	2 to 5 mm
Initial Particle Velocity	0.01 m/s
Initial Particle Temperature	20 C min, 100 C max
Initial Wall Temperature	100 C
Simulation Time Step	1 x 10^{-6}s

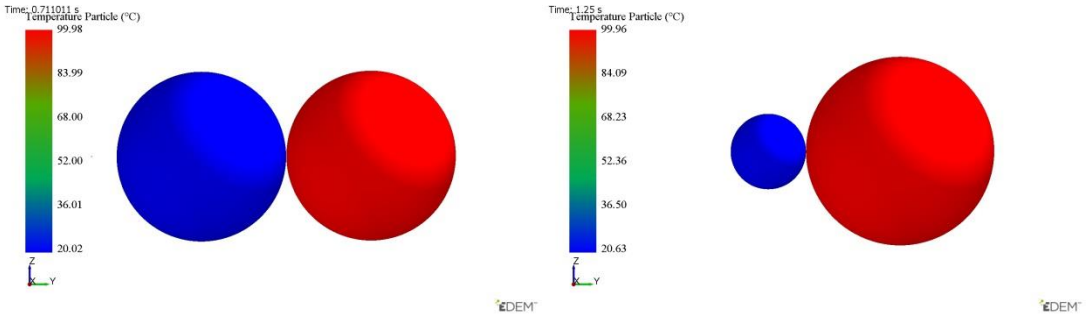

Figure 3 DEM results at the point of physical contact for size ratios 1 and 0.4

Particle-Wall Collisions

A similar simulation was used to investigate particle-wall collisions. A single particle collision at low velocity with a fixed surface was simulated for different particle sizes. Again, because the collision force was minimal the physical contact could be neglected. The gas film coefficient was calculated from the predicted heat flux and temperature difference.

RESULTS

Particle-Particle Collisions

The heat transfer coefficient (HTC) computed from the DEM simulations can be plotted as a function of the particle surface to surface distance normalized by the film thickness. The result is shown in Figure 4a. For a normalized separation distance of 1 there is no gas film contact and the coefficient is 0 for gas film conduction as expected. For values less than 1 the heat transfer coefficient increases logarithmically until the point of contact when the normalized separation distance is 0. For particle-particle collisions a set of curves was generated for the different particle size ratios. As the ratio approaches 0.4 the log curve becomes more acute nearest to the point of physical contact. At the point of contact a similar curve can be generated using the results for each particle size (Figure 5a). The response surface as a function of particle size and separation distance is shown in Fig 5b. The logarithmic relationship of the HTC to normalized separation distance is easily recognizable and the relationship between size ratio at the point of contact can also be seen.

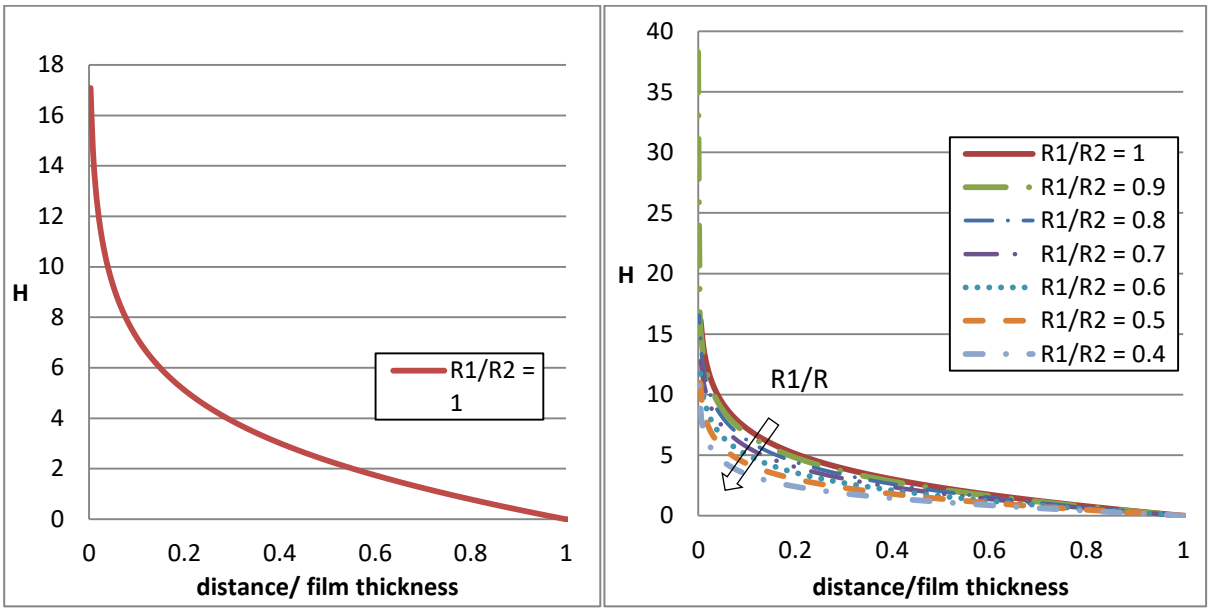

Figure 4a (left) Plot of the gas film coefficient vs the normalized separation distance for particle-particle size ratio = 1. **Figure 4b** (right) Gas film coefficient for different particle size ratios

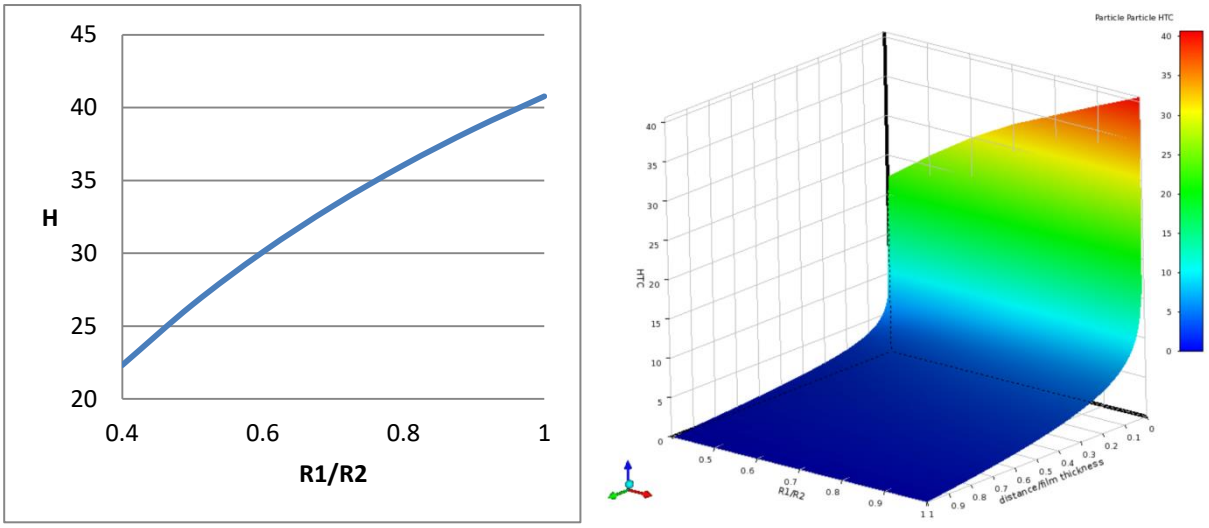

Figure 5a (left) Plot of gas film coefficient at the point of physical contact as a function of the particle size ratio. **Figure 5b** (right) Response surface for particle-particle gas film coefficient

This graphical representation of the HTC provides a much more intuitive description of the gas film heat transfer behavior involving particle-particle collisions. Curve fitting was used to describe the HTC relationships for film contact and physical contact in simple equations as follows:

Film Contact $$Q_{pfp} = \frac{R1/R2}{(R1/R2)^{0.2125}}\left[-3.161\ln\left(\frac{distance}{film\ thickness}\right) + 0.151\right]R_p k_f \Delta T \qquad (8)$$

$$\text{Physical Contact} \quad Q_{pfp} = [20.22\ln(R1/R2) + 40.604]\, R_p k_f \Delta T \tag{9}$$

where a weighting function using the size ratio (R1/R2) was determined to provide the best fit to describe the whole domain.

Particle-Wall Collisions

For particle-wall collision the curve for the heat transfer coefficient is simply a function of the particle size and the separation distance. Because we assume that the wall is infinite the shape of the curve is not affected by the particle size as shown in Figure 6a, that is, the curves for all the particle sizes are identical except for at the point of physical contact. At point of contact, the HTC shows an increasing with the particle size (as shown in Figure 6b). Curve fitting to each of these curves leads to Equations 10 and 11 respectively:

$$\text{Film Contact} \quad Q_{pfw} = \left[-6.101\ln\left(\frac{distance}{film\ thickness}\right) + 0.6015\right] R_p \mathrm{k}_f \Delta T \tag{10}$$

$$\text{Physical Contact} \quad Q_{pfw} = \left[6.2831\ln(R_p) + 110.17\right] R_p k_f \Delta T \tag{11}$$

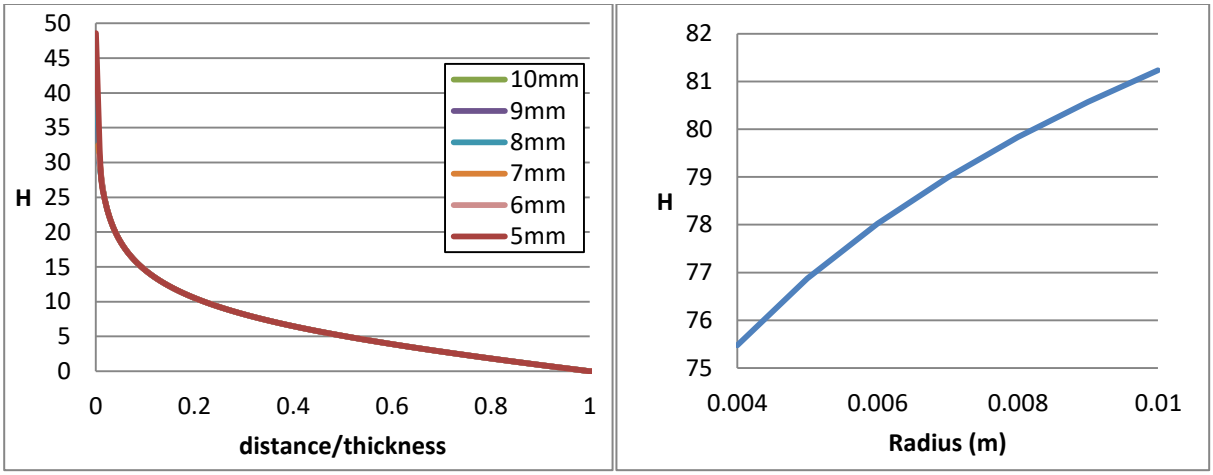

Figure 6a (left) Plot of particle-wall heat transfer coefficient for film contact. **Figure 6b** (right) Plot of particle-wall coefficient for physical contact as a function of particle radius.

Simplified Model for Gas Film Conduction Model

With the description of the heat transfer coefficient as a function of the normalized separation distance and particle size ratio, the gas film conduction model can be expressed in four simple equations 8-12. These equations were implemented in EDEM replacing the analytical solution to the

Rong integral. The computed HTC for particle-particle and particle-wall collisions using the simplified model are compared with the Rong/Morris full analytical mode in Figures 7 and 8 below which show an excellent agreement.

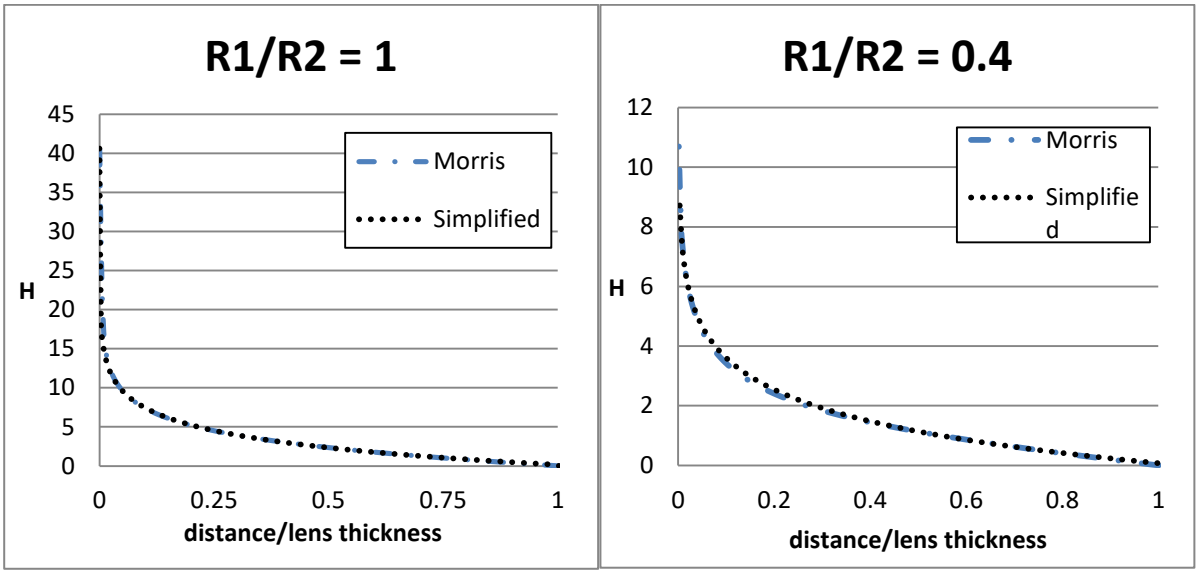

Figure 7 *Comparison of particle-fluid-particle coefficient for size ratio of 1 (left) and 0.4 (right)*

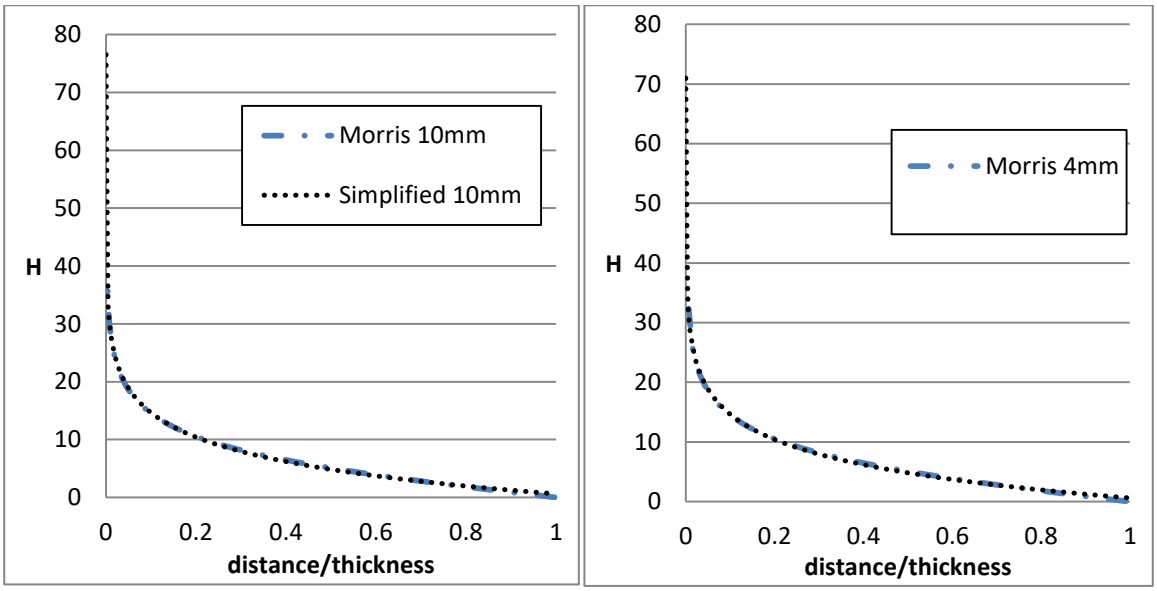

Figure 8 Comparison of particle-fluid-wall coefficient for size ratio of 10mm (left) and 4mm (right) particles

Further, comparing the computation time of the calculation for a single binary collision, the portion of time spent on the conduction calculation can be determined by subtracting the calculation time of the standard Hertz-Mindlin model with no conduction from the total time. Figure 9 shows that 27% of the total calculation time was spent on the Morris conduction calculation while only 19% of

the total time was spent on the simplified model. This represents an improvement of 33.4% of the conduction calculation. The net total improvement is approximately 9.0%. Further tests of an industrial scale problem with 250,000 particles have demonstrated speed improvements of 10% with near identical results for particle temperature (Figure 10). In this mill test case with heated walls, the maximum particle temperature after 10 second of simulation time for the simplified model is within 0.022% of the maximum value predicted by the Morris model and the maximum gas film heat flux within 0.0017% of the Morris model. The improvement in calculation time will depend on the individual simulation, but results for a range of simulations have been between 5 and 15% with simulations with more static contacts showing the least benefit.

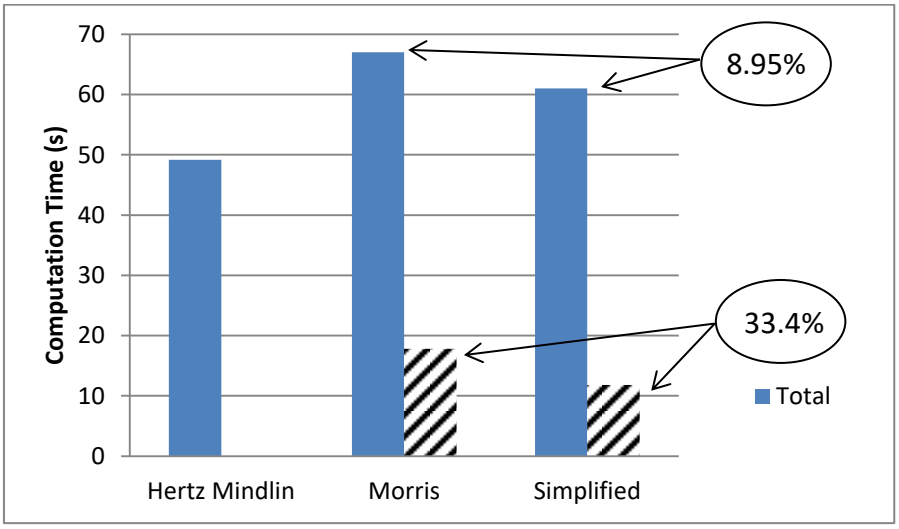

Figure 9 Computation time for standard Hertz Mindlin with no conduction, Morris gas film, and the Simplified conduction model for a binary collision

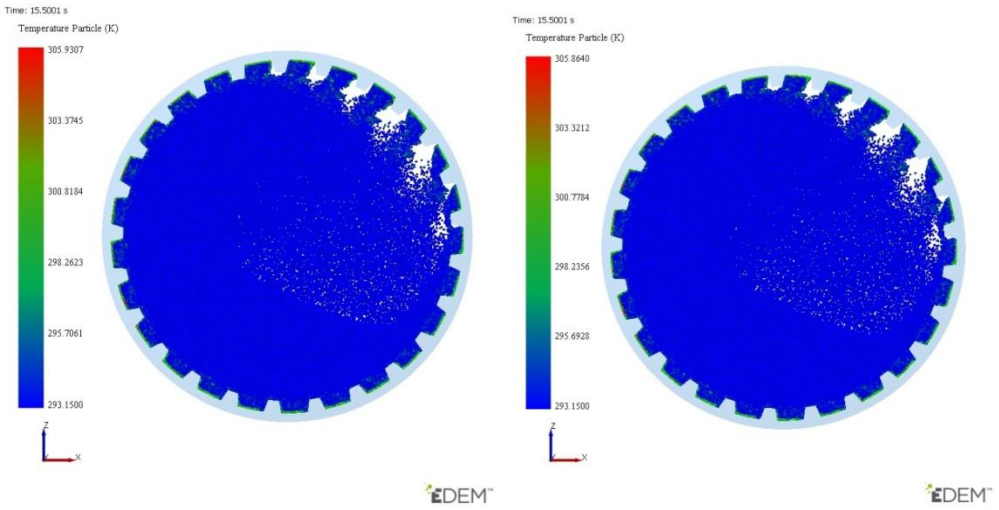

Figure 10. Particle temperature for mill test case with 250,000 particles. The Morris model is on the left, the simplified model on the right.

CONCLUSION

In this study we have investigated the behavior of particle scale gas film conduction for particle-particle and particle-wall contacts. Using a model proposed by Rong as implemented by Morris, DEM simulations were carried out for a binary collision and a single particle-wall collision using a range of particle sizes. The heat transfer coefficient was calculated based on the simulation results and plotted against normalized separation distance. The heat transfer coefficient is found to vary logarithmically with separation distance and simple models were proposed from best fit to the simulation results.

This simplified model was shown to reduce the total computation time of a range of flow regimes in the order of 5 to 15%. It should be noted that since the curve fits are based on results up to the point of contact with no overlap, this model is independent of particle overlap which is advantageous when a reduced material stiffness is used to speed up calculations. Beyond computational efficiency, the simpler expression for the relationship of the gas film coefficient will be useful in the next stage of work investigating scaling laws and the impact of the gas film model on multi-sphered particles.

Acknowledgements

The authors are grateful to Astec, Inc. for funding this research and to DEM Solutions staff, especially Christophe Le Dauphine and Carles Bosch Padros as well as to Aaron Morris whose work serves as the basis for this investigation.

REFERENCES

[1] Cundall, P.A. and Strack, O.D., 1979. A discrete numerical model for granular assemblies. Geotechnique, 29(1), pp.47-65.

[2] Kremmer, M. and Favier, J.F., 2001. A method for representing boundaries in discrete element modelling – part I: Geometry and contact detection, *Int. J. Numerical Methods in Engineering*, 51, 1407-1421.

[3] Kremmer, M. and Favier, J.F., 2001. A method for representing boundaries in discrete element modelling – part II: Kinematics, *Int. J. Numerical Methods in Engineering*, 51, 1423-1436.

[4] Brosh, T. and Levy, A., 2010. Modeling of heat transfer in pneumatic conveyer using a combined DEM-CFD numerical code. Drying Technology, 28(2), pp.155-164.

[5] Chaudhuri, B., Muzzio, F.J. and Tomassone, M.S., 2006. Modeling of heat transfer in granular flow in rotating vessels. Chemical Engineering Science, 61(19), pp.6348-6360.

[6] Li, J. and Mason, D.J., 2002. Application of the discrete element modelling in air drying of particulate solids. Drying Technology, 20(2), pp.255-282.

[7] Hobbs, A., 2009. Simulation of an aggregate dryer using coupled CFD and DEM methods. International Journal of Computational Fluid Dynamics, 23(2), pp.199-207.

[8] Batchelor, G.K. and O'brien, R.W., 1977, July. Thermal or electrical conduction through a granular material. In Proceedings of the Royal Society of London A: Mathematical, Physical and Engineering Sciences (Vol. 355, No. 1682, pp. 313-333). The Royal Society.

[9] Rong, D. and Horio, M., 1999, December. DEM simulation of char combustion in a fluidized bed. In Second International Conference on CFD in the Minerals and Process Industries CSIRO, Melbourne, Australia (pp. 65-70).

[10] D. Rong, DEM Simulation of Hydrodynamics, Heat Transfer and Combustion in Fluidized Beds, Ph.D. thesis, Tokyo University of Agriculture and Technology, Tokyo, Japan, 2000.

[11] Bu, C.S., Liu, D.Y., Chen, X.P., Liang, C., Duan, Y.F. and Duan, L.B., 2013. Modeling and Coupling Particle Scale Heat Transfer with DEM through Heat Transfer Mechanisms. *Numerical Heat Transfer, Part A: Applications*, *64*(1), pp.56-71.

[12] Morris, A.B., Pannala, S., Ma, Z. and Hrenya, C.M., 2015. A conductive heat transfer model for particle flows over immersed surfaces. *International Journal of Heat and Mass Transfer*, *89*, pp.1277-1289

[13] Syamlal, M., Rogers, W., & O'Brien, T. J. 1993. MFIX documentation: Theory guide. *National Energy Technology Laboratory, Department of Energy, Technical Note DOE/METC-95/1013 and NTIS/DE95000031*.

[14] DEM Solutions, Ltd., 2015 EDEM 2.7 Programming Guide, Online.